ELSEVIER

Biochimica et Biophysica Acta 1415 (1998) 147–162

BIOCHIMICA ET BIOPHYSICA ACTA
BBA

Mechanical aspects of membrane thermodynamics. Estimation of the mechanical properties of lipid membranes close to the chain melting transition from calorimetry

Thomas Heimburg *

Max-Planck-Institut für biophysikalische Chemie, AG Membrane Thermodynamics, Am Fassberg 11, 37077 Göttingen, Germany

Received 16 July 1998; accepted 2 October 1998

Abstract

Changes in the internal energy of lipids with temperature are related to both lipid volume and area changes. Close to the chain melting transition of lipid bilayers volume and enthalpy fluctuations generally follow proportional functions. This makes it possible to calculate the relationship between membrane excess heat capacity with lipid volume, area compressibility and the membrane bending modulus, if the area fluctuations of the two monolayers are assumed to be mainly decoupled. Thus, compressibility and elasticity display pronounced maxima at the chain melting transition. These maxima can also be related to pronounced minima of the sound velocity in the lipid transition range, which were found in ultrasonic experiments. In the present study heat capacity profiles and volume changes were obtained. The compressibilities and the bending modulus were then deduced from the specific heat. The relevance of these findings for structural transitions and for the curvature dependence of heat capacities is discussed.

Keywords: Compressibility; Elasticity; Sound velocity; Heat capacity

1. Introduction

Membrane morphologies are closely linked to the elastic properties of the bilayer. In the last few decades many groups have been involved in the determination of the elastic properties of artificial [1,2] and biological membranes [3–5]. In the thermotropic chain melting transition, pronounced maxima of the mechanical susceptibilities were found [6–9]. Simultaneously, a variety of studies have focused on the understanding of the chain melting process and the analysis of heat capacity profiles by statistical thermodynamics means. Simulations of lipid phase transitions at the molecular level have gained increasing attention [10–14]. The main focus of these studies was the understanding of the lipid mixing behavior in systems with several components, based on lattice models including nearest neighbor interactions. Examples are binary mixtures [15,16], and membranes containing integral proteins [17–21] or cholesterol [22]. The fluctuation theorem allows for the calcula-

Abbreviations: C_p, specific heat capacity at constant pressure; DMPC, 1,2-dimyristoyl-*sn*-glycero-3-phosphocholine; DPPC, 1,2-dipalmitoyl-*sn*-glycero-3-phosphocholine; DMPG, 1,2-dimyristoyl-*sn*-glycero-3-phosphoglycerol; EDTA, ethylenediaminetetraacetic acid; HEPES, *N*-(2-hydroyethyl)piperazine-*N'*-2-ethanesulfonic acid; LUV, large unilamellar vesicles; MLV, multilamellar vesicles; HWHH, half width at half height; ΔH, excess transition enthalpy

* WWW: http://www.gwdg.de/~theimbu;
E-mail: theimbu@gwdg.de

0005-2736/98/$ – see front matter
PII: S0005-2736(98)00189-8

tion of the heat capacity from the distribution of states in an equilibrium Monte-Carlo simulation [23]. Enthalpy fluctuations in membranes are maximized in the chain melting regime resulting in a pronounced heat capacity maximum. Most of these studies have concentrated on lipid monolayers, but some studies have also examined bilayer membranes, using a state function including the lipids of both sides of the membrane [14]. Within the framework of these models, fluctuations are linked to a microheterogeneity of the lipid state and the composition within the membrane plane [24].

Several of the earlier studies described volume changes in the melting transition [6,25–27]. The average volume of a DPPC lipid membrane, for example, changes by about 4% upon melting [26]. The lipid area simultaneously changes by 25% [8]. Thus, dimensional changes are much more pronounced in the membrane plane than in the overall volume. Since enthalpy, volume and temperature change in the same temperature regime, one may expect that volume and area fluctuations in membranes also increase in the transition range. Volume and area fluctuations, however, are known to be related to volume and area isothermal compressibilities, respectively [28]. The coupling between enthalpy and volume fluctuations is the subject of this paper.

Since the classical paper of Helfrich [29], derived from liquid crystal elastic theory [30], many studies have focused on the elastic properties of membranes and the coupling to vesicular shapes. Changes in the elastic constants may give rise to surface curvature undulations [31–33] and may also result in structural or shape transitions [3,34,35]. Depending on the elastic constants a variety of shapes may minimize the energy of closed vesicles, and explain the many possible shapes in erythrocytes [36].

In this paper we couple membrane fluctuations in area, volume and curvature in order to derive simple relations between volume and area isothermal and adiabatic compressibilities with the heat capacity. The knowledge of these parameters is then used to calculate the membrane elasticity and to rationalize the temperature dependence of the sound velocity of lipid dispersions. Finally, we will argue that close to melting transitions structural transitions in vesicles may occur if a competition between an external force and the bending elasticity exists as is the case in vesicles under osmotic stress. We predict that these transitions will be visible in the specific heat profile.

2. Materials and methods

Dipalmitoyl phosphocholine (DPPC, Avanti Polar Lipids, Birmingham, AL) was used without further purification. Multilamellar vesicles (MLV) were obtained by preparing dispersions in buffer (2 mM HEPES, 1 mM EDTA, pH 7.5) or in distilled water. The dispersion was vortexed above the lipid melting point until the solution appeared to be homogeneous. Large unilamellar vesicles (LUV) were prepared from the MLV dispersions by extrusion, using an extruder (Avestin Inc., Ottawa, Canada) with a filter pore size of about 100 nm. Alternatively, LUV were prepared by ultrasonication of the MLV dispersion and subsequent incubation of the dispersions below the melting point (at room temperature) for about 4 weeks.

Calorimetric experiments were performed on a MicroCal (Northampton, MA) MC2 differential scanning calorimeter with scan rates of 1°/h and 5°/h, respectively.

The densitometric experiment was performed on two coupled DMA 602 vibrating tube densitometers by Anton Paar (Graz, Austria) with a lipid dispersion in one cell and the reference buffer in the second cell. This procedure allowed for the correction of time dependent drifts, resulting in high data accuracy. Details will be published in a paper giving in addition the details of the set of experimental data presented in Fig. 1 (Ebel and Heimburg, unpublished).

2.1. Theory

The enthalpy of a membrane is given by the time or spatial average over all available states. These membrane states may differ in the number of lipids in the available single lipid substates and in their lateral arrangement in the lipid matrix:

$$H_i \equiv E_i + pV_i + \Pi A_i \quad (1)$$

with E_i being the internal energy of the bilayer in state i, V_i being the volume and A_i the area. H_i can be considered the Hamiltonian energy in a sys-

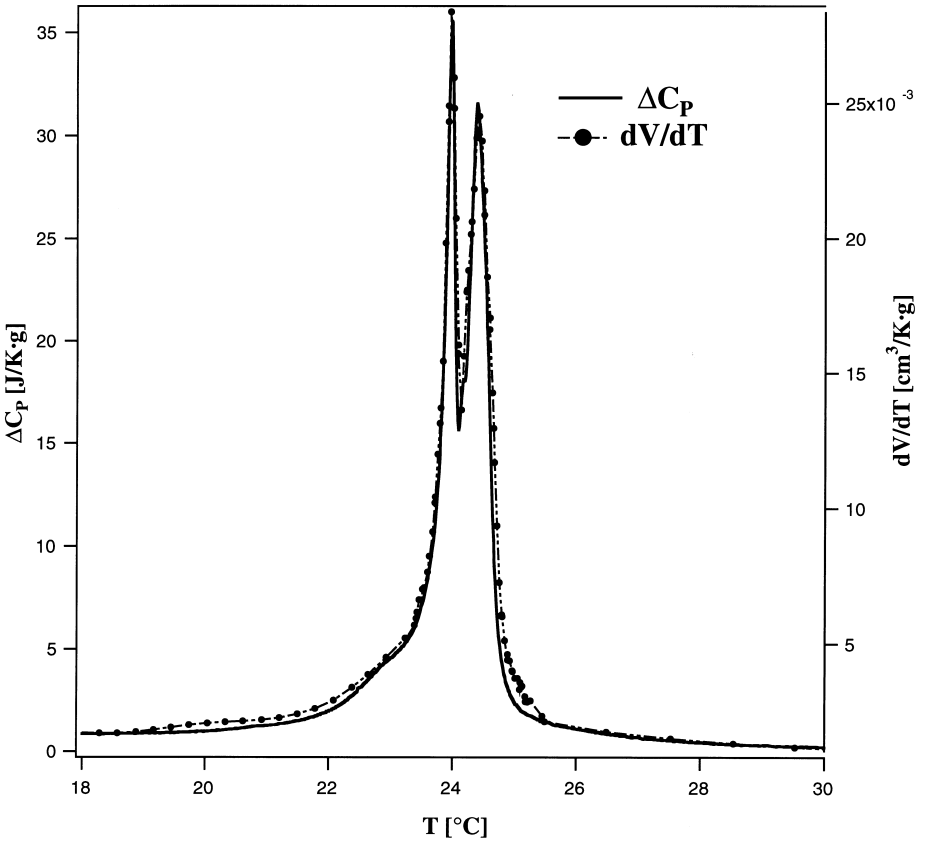

Fig. 1. Proportionality of volume and heat. Heat capacity profile of the main transition of extruded DMPC vesicles in comparison with the temperature dependence of the specific volume (detailed view of unpublished data from H. Ebel, Göttingen, with permission). The heat capacity profile displays two peaks. The volume expansion coefficient is nearly superimposible with the C_p profile, even in minute details of the temperature profiles.

tem with constant static and lateral pressures p and Π. The magnitude of E_i, V_i and A_i can be modeled in statistical mechanics calculations, as has been done for example by Zhang et al. [14] and Mouritsen [12,13]. The interaction energies in these models contain the internal energies of the individual lipids and the nearest neighbor lipid-lipid interaction energies.

The partition function for a monolayer at constant pressure and constant temperature is given by:

$$Q = \sum_i \Omega_i \exp\left(-\frac{H_i}{RT}\right). \tag{2}$$

This is the so-called Guggenheim partition function for isothermal, isopiestic conditions [28,37], modified for the boundary condition of constant lateral pressure. Ω_i is the degeneracy of states with identical Hamiltonian energies.

The observables $\overline{X}$ are average values defined by:

$$\overline{X} = \frac{1}{Q} \cdot \sum_i X_i \cdot \Omega_i \exp\left(-\frac{H_i}{RT}\right), \tag{3}$$

where X_i may be H_i, V_i or A_i. By differentiating the enthalpy $\overline{H}$ as defined in Eq. 3 with respect to T, $\overline{V}$ with respect to p, and $\overline{A}$ with respect to Π, one obtains the susceptibilities, namely the heat capacity at constant pressure, C_p, and the isothermal volume and area compressibilities, κ_T^{vol} and κ_T^{area}, respectively:

$$C_P = \left.\frac{d\overline{H}}{dT}\right|_P = \frac{\overline{H^2} - \overline{H}^2}{RT^2}, \quad \kappa_T^{vol} = -\frac{1}{\overline{V}} \cdot \left.\frac{d\overline{V}}{dp}\right|_T =$$

$$\frac{\overline{V^2} - \overline{V}^2}{\overline{V} \cdot RT}, \text{ and } \kappa_T^{area} = -\frac{1}{\overline{A}} \cdot \left.\frac{d\overline{A}}{d\Pi}\right|_T = \frac{\overline{A^2} - \overline{A}^2}{\overline{A} \cdot RT}, \tag{4}$$

thus coupling the susceptibilities with the fluctuations of the system [28].

Let $H_0(T)$ be the intrinsic heat of the membrane lipids and $\Delta H(T)$ be the excess heat linked to the chain isomerizations. The heat capacity is then given by

$$C_P = \left.\frac{dH_0}{dT}\right|_P + \left.\frac{d(\Delta H)}{dT}\right|_P = C_{P,0} + \Delta C_P \tag{5}$$

with ΔC_P being the excess heat capacity. Similarly, if $V_0(T)$ is the intrinsic volume of the membrane lipids and $\Delta V(T)$ is the excess volume change, one obtains

$$\kappa_T^{vol}(T) = -\left.\frac{1}{V}\frac{dV_0}{dp}\right|_T - \left.\frac{1}{V}\frac{d(\Delta V)}{dp}\right|_T = \kappa_{T,0}^{vol} + \Delta\kappa_T^{vol} \ . \tag{6}$$

$\kappa_{T,0}^{vol}$ is the intrinsic volume compressibility of the lipids at a given temperature T, being related to the volume fluctuations at the molecular level which are unrelated to changes in the physical state. $\Delta\kappa_T^{vol}$ is the volume 'excess' compressibility, linked to fluctuation in the membrane state. $\kappa_{T,0}^{vol}$ may adopt different values above and below the transition, accounting for the fact that the isothermal compressibilities in the gel state of a lipid membrane are lower than in the liquid crystalline phase [6].

Similarly for the area compressibility one obtains

$$\kappa_T^{area}(T) = -\left.\frac{1}{A}\frac{dA_0}{d\Pi}\right|_T - \left.\frac{1}{A}\frac{d(\Delta A)}{d\Pi}\right|_T = \kappa_{T,0}^{area}(T) + \Delta\kappa_T^{area}(T). \tag{7}$$

The first term on the right-hand side consists in the intrinsic compressibility of a lipid membrane in a given state at temperature T. The second term is the lateral 'excess' compressibility, linked to the fluctuations in the membrane state.

Using the Maxwell relations one can demonstrate that both the adiabatic volume and area compressibilities can be expressed as a function of isothermal compressibility, heat capacity and the temperature dependence of volume or area [38]. In the absence of lateral stress one obtains for the adiabatic volume compressibility

$$\kappa_S^{vol} = \kappa_T^{vol} - \frac{T}{\overline{V}\cdot C_P}\left(\frac{d\overline{V}}{dT}\right)_P^2. \tag{8}$$

Similarly at constant bulk pressure, p, one obtains for the two-dimensional adiabatic compressibility, κ_S^{area}

$$\kappa_S^{area} = \kappa_T^{area} - \frac{T}{\overline{A}\cdot C_\Pi}\left(\frac{d\overline{A}}{dT}\right)_\Pi^2, \tag{9}$$

where C_Π is the heat capacity at constant lateral tension, equal to the bulk heat capacity C_P as in Eq. 8.

In principle, isothermal compressibility, heat capacity and volume expansion coefficient are independent functions, and no simple macroscopic relation between them exists. Thus, all three functions have to be determined in independent experiments to fully describe the thermodynamic and mechanical properties of the system.

2.2. Isothermal volume and area compressibilities close to the main transition

In this section, we will demonstrate that in the special case of lipid membranes it is possible to derive some simple relations between the excess heat capacity and the compressibilities, which are applicable in the lipid chain melting regime.

It is known that both volume and area undergo significant changes in the melting regime. This is mainly related to trans-gauche isomerizations of the lipid chains. The temperature dependence of the volume (or area) depends on both intrinsic volume changes of each molecule in a given state and state changes of individual molecules which cause the discontinuity in the melting regime.

The enthalpy of lipids in the chain melting regime is given by $\overline{H(T)} = \overline{H_0} + \overline{\Delta H}$. Anthony et al. [27] showed by densitometry that the enthalpy change (the excess heat), ΔH, and the relative volume change (the excess volume), ΔV, are proportional functions in the lipid melting transition range:

$$\overline{\Delta V(T)} = \gamma_{vol}\cdot\overline{\Delta H(T)}. \tag{10}$$

This relation was also found to be true in lipid mix-

tures over a wide temperature range. Further experimental evidence supporting this point is given in the results section of this paper (Fig. 1), demonstrating that this relation is even true for minute details in the melting curve with complex melting behavior.

Consequently,

$$\frac{d(\overline{\Delta V})}{dT} = \gamma_{\mathrm{vol}} \frac{d(\overline{\Delta H})}{dT} = \gamma_{\mathrm{vol}} \Delta C_{\mathrm{P}}. \tag{11}$$

If Eq. 10 is true in a wide temperature interval, it can be shown that not only $\overline{\Delta V} = \gamma_{\mathrm{vol}} \overline{\Delta H}$, but also that $\Delta V_{\mathrm{i}} = \gamma_{\mathrm{vol}} \Delta H_{\mathrm{i}}$ for each available (relevant) substate. This implies that $\overline{\Delta V^2} = \gamma_{\mathrm{vol}}^2 \cdot \overline{\Delta H^2}$ (see Appendix A for derivation). Using Eqs. 4 and 6 one can calculate the 'excess' compressibility

$$\Delta \kappa_{\mathrm{T}}^{\mathrm{vol}} = \frac{\gamma_{\mathrm{vol}}^2 T}{\overline{V}} \Delta C_{\mathrm{P}}. \tag{12}$$

Therefore, the temperature dependence of the 'excess' isothermal compressibility is a simple function of the heat capacity change in the transition. Thus, both quantities display pronounced maxima in the melting regime.

The isothermal volume compressibility can be approximated using a simple function of the heat capacity. This conclusion was drawn above because of the proportionality of the enthalpy and volume change close to the melting transition. Unfortunately, no such detailed information is available for the membrane area. However, it is known that the area of a lipid membrane in the melting transition changes considerably. Based on a papers by Rand and Parsegian [39], Needham and Evans [8] and Nagle et al. [56] we assume in the following calculation a relative area change of 24.6% (see Section 4 for details). Taking this together with the finding that $\Delta V_{\mathrm{i}} = \gamma_{\mathrm{vol}} \Delta H_{\mathrm{i}}$ for all relevant substates of the partition function, it is plausible to postulate a proportionality relation between heat and area as well. With this assumption we can approximate the lateral compressibility by:

$$\Delta \kappa_{\mathrm{T}}^{\mathrm{area}} = \frac{\gamma_{\mathrm{area}}^2 T}{A} \Delta C_{\mathrm{P}}, \tag{13}$$

where $\Delta \kappa_{\mathrm{T}}^{\mathrm{area}}$ is the lateral 'excess' compressibility.

2.3. Isothermal membrane elasticity close to the main transition

One may envisage the membrane bending elasticity in terms of the lateral compressibility of the membrane monolayers. Upon bending the membrane, the outer monolayer is expanded whereas the inner monolayer is compressed. Evans [40] derived the following expression for the bending modulus K_{bend} of an isotropic bilayer with symmetric monolayers

$$\frac{1}{K_{\mathrm{bend}}} \equiv \kappa_{\mathrm{bend}} = \frac{2 \cdot \kappa_{\mathrm{T}}^{\mathrm{monolayer}}}{h^2}, \tag{14}$$

where $\kappa_{\mathrm{T}}^{\mathrm{monolayer}}$ is the lateral compressibility of a monolayer, and h is the distance of the two monolayers. Taking the lateral compressibility of a bilayer to be half the compressibility of a monolayer and the distance between the monolayers to be the distance between the monolayer centers ($h = D/2$), one arrives at

$$\kappa_{\mathrm{bend}} = \frac{16 \cdot \kappa_{\mathrm{T}}^{\mathrm{area}}}{D^2}. \tag{15}$$

This assumes that the fluctuations in the two monolayers are mainly decoupled. Taking the thickness values from the literature for DMPC membranes in the fluid state ($D = 35.5$ Å, [2]) and compressibility ($\kappa_{\mathrm{T}}^{\mathrm{area}} = 7.5$ m/N, [7]) yields $\kappa_{\mathrm{bend}} = 9.52 \times 10^{18}$ J^{-1} ($K_{\mathrm{bend}} = 1.05 \times 10^{-19}$ J), which is close to the experimental value for the bending elasticity of DMPC in the fluid phase ($K_{\mathrm{bend}} = 1.1 \times 10^{-19}$ J at $T = T_{\mathrm{m}} + 2.5°$ [5]).

Thus, within this simple framework, the 'excess' bending elasticity close to the transition is a simple function of the heat capacity, as are the lateral and volume compressibility,

$$\kappa_{\mathrm{bend}} = \kappa_{\mathrm{bend},0}(\mathrm{T}) + \eta \Delta C_{\mathrm{P}}, \tag{16}$$

with $\Delta \kappa_{\mathrm{bend}}$ being the 'excess bending elasticity' and $\eta = 16\ \gamma_{\mathrm{area}}^2 T / D^2 A$.

As mentioned, this approximation is only true if the fluctuations of the two monolayers are decoupled. The limitations of this approach will be discussed in Section 4.

2.4. Adiabatic compressibilities close to the main transition

The adiabatic volume compressibility, κ_S^{vol}, may now be obtained by introducing Eqs. 10–12 into Eq. 8. When calculating the κ_S^{vol} of aqueous lipid dispersions, one has to take into account that the specific functions X ($X = C_p$, κ_T, V, dV/dT) are average values, given by $X = f_{H_2O} \cdot X_{H_2O} + f_{lipid} \cdot X_{lipid}$, where f_{H_2O} and f_{lipid} are the water and lipid fractions, respectively. The values of V and C_p for water can be found in the Handbook for Physics and Chemistry [41]. The isothermal compressibility of H_2O is given by Beggerow [42].

The heat capacity C_p is that of the overall system. C_p may vary between ΔC_P and infinity, depending on the absolute water content of the sample. Physically, this means that the heat produced by the lipid chain transitions upon compression, ΔH, must be absorbed by the environment with a heat capacity $C_P > \Delta C_P$ to result in a measurable adiabatic compressibility. The larger the heat buffering capacity of the environment, the larger is the adiabatic compressibility. In the limiting case of complete relaxation and large water content, the adiabatic compressibility of the membranes is similar to the isothermal compressibility, since the second term in Eq. 8 disappears.

Lipid dispersions, however, are special with respect to the discontinuous features of the system. Close to the melting transition the majority of the heat is released locally within the membrane. If the measurement is not infinitely slow, the heat redistribution is not complete, due to the finite time constants of relaxation processes. The buffer that absorbs the released heat is just as big as the volume accessible by relaxation or heat conduction within the finite time τ. Therefore for time-dependent processes in Eq. 8 one should rather consider an effective buffering heat capacity $C_p^{eff}(\tau) < C_p$ that depends on time dependence of compression and on the relaxation time constant τ. This has been reviewed by van Osdol et al. [43].

Typical determinations of ultrasonic velocities, for example, are performed at frequencies in the kiloHertz to gigaHertz regime. Relaxation times of lipid membranes, however, may be considerably slower, down to the second regime at the chain melting point, as measured by volume perturbation calorimetry [44]. This implies that heat redistribution in an ultrasonic experiment is not complete and that the adiabatic compressibility determined from this experiment is lower than that in the limit of a frequency approaching zero.

If relaxation is so slow, one may consider the membranes and the buffer as being adiabatically decoupled in the high frequency regime. No heat will be transferred from the membranes to the buffer and vice versa.

Under these circumstances, the adiabatic compressibilities of the buffer and the lipids are additive:

$$\kappa_S^{vol} = f_{H_2O} \cdot \kappa_{S,H_2O}^{vol} + f_{lipid} \cdot \kappa_{S,lipid}^{vol} \tag{17}$$

with f_{H_2O} and f_{lipid} being the volume fractions of water and lipid.

The adiabatic lipid compressibility may now be approximated by

$$\kappa_{S,lipid}^{vol} = \kappa_{T,0}^{vol,lipid} + \Delta\kappa_T^{vol} - \frac{T}{\overline{V}^{lipid} \cdot C_P^{lipid}} \left(\frac{d\overline{V}^{lipid}}{dT} \right)_P^2 . \tag{18}$$

If the volume expansion coefficient of the lipid chains is neglected, $dV/dT = \gamma \cdot \Delta C_P$, and

$$\kappa_{S,lipid}^{vol} \approx \kappa_{T,0}^{vol,lipid} + \Delta\kappa_T^{vol} \left(1 - \frac{\Delta C_P}{C_P^{lipid}} \right) . \tag{19}$$

At high frequencies ($\tau \to 0$), heat cannot be absorbed by the environment ($C_p = \Delta C_p$) and the lipid state fluctuation-related term in adiabatic compressibility is zero.

As discussed below, this approach seems to be successful for lipid vesicles in the transition regime at high ultrasonic excitation frequencies.

3. Results

The basis of the theoretical treatment in this paper is the proportional relation between volume and enthalpy in the chain melting transition. This finding was reported by Anthony et al. [27]. Fig. 1 displays the heat capacity profile of extruded dimyristoyl phosphatidylcholine (DMPC) vesicles, which were obtained using high sensitivity differential scanning

calorimetry (DSC). They display two peaks in the melting regime. Superimposed is the specific volume expansion coefficient dV/dT, deduced from the analytical derivative of a specific volume profile as obtained from a high sensitivity densitometer (I am grateful to H. Ebel from our lab for letting me use this set of data prior to detailed publication). Perfect superimposition of the two curves was found. Extruded DMPC vesicles have been shown to display two peaks in the melting regime [45,46]. This splitting of the peaks is a consequence of the extrusion process and is probably linked to structural transitions in the vesicles [46]. The perfect matching of the heat capacity and the volume expansion coefficient demonstrates that the proportionality relation between heat and volume is true for all aspects of the melting process. A proportionality factor $\gamma^{vol} = 7.721 \times 10^{-4}$ cm^3/J was found.

The importance of the preparation process of the lipid dispersions is demonstrated in Fig. 2. Experimental heat capacity profiles of three different dipalmitoyl phosphatidylcholine (DPPC) vesicle preparations were compared, as are MLV (Fig. 2a,b top) and LUV, the latter being prepared either by extrusion (Fig. 2a,b center) or by sonication (Fig. 2a,b bottom). The three profiles are different with respect to the exact melting temperature and to the cooperativity of the transition. The multilamellar vesicles displayed a very pronounced heat capacity maximum of 456 kJ/mol·deg, whereas the extruded unilamellar vesicles had 45.1 kJ/mol·deg and the sonicated vesicles 13.2 kJ/mol·deg. The integrated area of the three profiles was roughly the same ($\Delta H_0 = 39.2$ kJ/mol including the pretransition for MLV). Due to the different transitional cooperativity, the multilamellar vesicle profiles display a transition half width at half height (HWHH) of about 0.05°, while the extruded vesicles had a HWHH = 0.55° and the sonicated vesicles had a HWHH = 1.50°. These findings imply that at the melting point the isothermal 'ex-

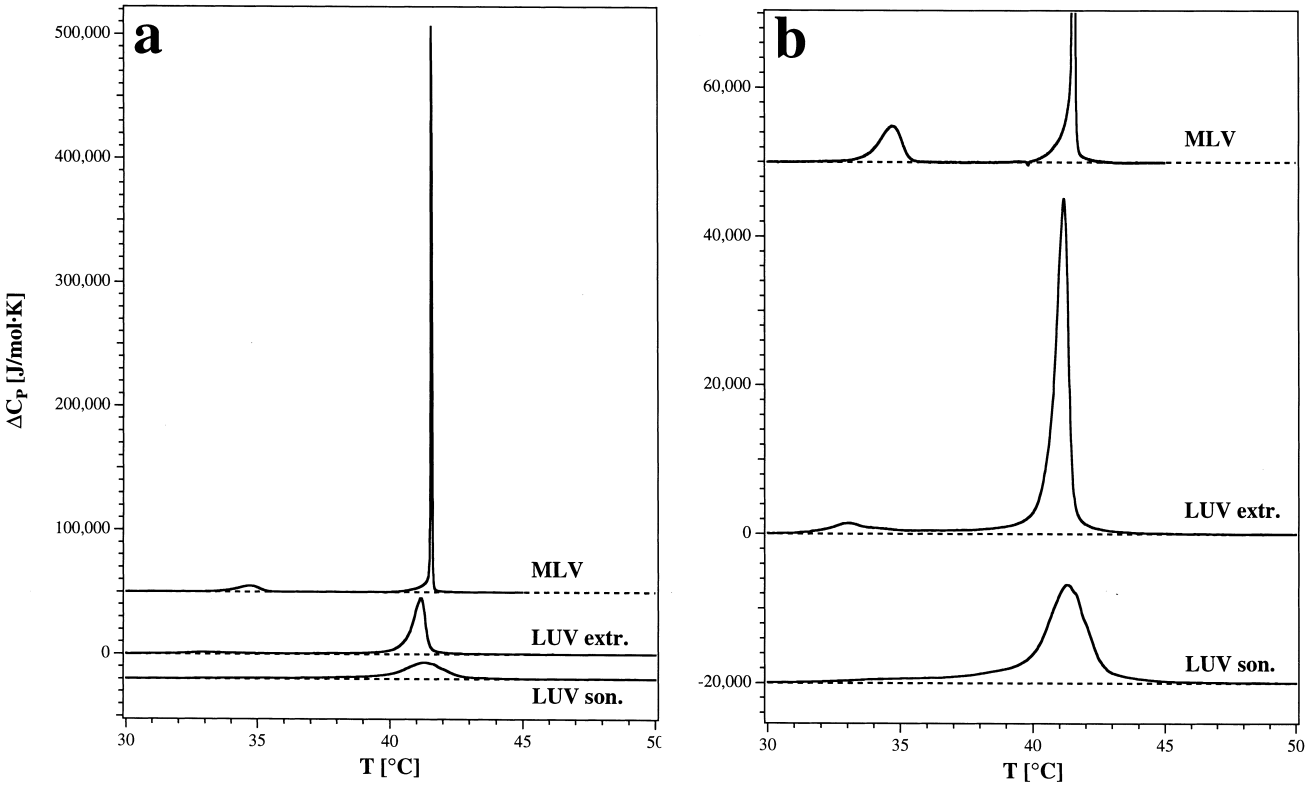

Fig. 2. Experimental heat capacity profiles for DPPC MLV (top), extruded DPPC LUV (center) and sonicated DPPC LUV (bottom). The MLV trace was recorded at 1°/h, the LUV traces at 5°/h. (a) Full traces. (b) Expanded view, showing an extreme difference in transition half width. Pre- and main transition are separated in the MLV scan but cannot be separated for the LUV.

cess' compressibility is 10 times higher in MLV than in extruded LUV and 35 times higher than in sonicated LUV.

In the MLV profile it is possible to separate the pretransition (formation of the ripple phase) from the main transition. The corresponding heat and volume changes are given in Table 1. Interestingly the ratio of the transition enthalpies and the volume

Table 1
Literature data of membrane parameters and elastic constants of DPPC

		Gel	Fluid
Calorimetry	heat capacity $C_{P,0}$ [J/mol·K]	**1600** (21.5°) [50]	**1650** (51.5°) [50]
	melting point main transition [°C]	**41.6**[a]	
	melting point pretransition [°C]	**34.7**[a]	
	excess heat main transition [kJ/mol]	**34.0** (multilayers)[a]	
	excess heat pretransition [kJ/mol]	**5.26** (multilayers)[a]	
Volume V	specific volume [cm^3/g]	0.947 (L_β', 33°) [26] 0.953 (P_β', 35°) **0.960** (P_β', 41.5°)	0.999 (L_α, 41.5°) [26] 1.004 (L_α, 45°) [63]
	rel. vol. change main transition $\Delta V/V$	**0.0406** ($P_\beta' \rightarrow L_\alpha$)[b]	
	rel. vol. change pretransition $\Delta V/V$	**0.0064** ($L_\beta' \rightarrow P_\beta'$)[b]	
	γ^{vol} main transition [cm^3/J]	$\mathbf{8.599\times10^{-4}}$[b]	
	γ^{vol} pretransition [cm^3/J]	$\mathbf{8.642\times10^{-4}}$[b]	
	intrinsic thermal volume expansion coefficient $V^{-1}\cdot(dV/dT)$ [K^{-1}]	**0.00088**[b] [26]	**0.001**[b] [26]
		($T <$ pretransition)	($T >$ main transit.)
	volume compressibility κ_T [m^3/J]	$< \sim 3.3\times10^{-11}$ [6] $\mathbf{5.2\times10^{-10}}$ [47]	$1.1\text{–}1.7\times10^{-9}$ [6] $\mathbf{7.8\times10^{-10}}$ [47]
Area A	area/lipid [Å^2]	**47.4** (L_β', 25°) [57] 50 (L_β', 30°) [52,53] 50.5 (P_β', 37°) 48.6 (L_β', 25°) [39]	**62.9** (L_α, 50°) [54,56] 58.2 (L_α, 45°) [53,54] 68.1 (L_α, 50°) [39]
	specific area [cm^2/g]	$\mathbf{1.90\times10^6}$[b] [57] (L_β', 25°)	$\mathbf{2.52\times10^6}$[b] [56] (L_α, 50°)
	rel. area change $\Delta A/A$	**0.246**[d] [56,57] [$P_\beta' \rightarrow L_\alpha$: 0.22[c] [8]]	
	γ^{area} [cm^2/J]	$\mathbf{8.93\times10^3}$ (with $\Delta A/A = 0.246$)[b]	
	intrinsic thermal area expansion coefficient $A^{-1}\cdot(dA/dT)$ [K^{-1}]	**0.0026** (25°C) [57] [0.0035[c] [8]]	[0.0042[c] [8]]
	area compressibility [m^2/J]	**1.0** (L_β', 25°) [39] [1.1 (8.3°C)[c] [8]]	**6.9** (L_α, 50°) [39] [7.5 (26°C)[c] [7]] [6.9 (29°C)[c] [8]]
	elasticity [J]	–	1.5×10^{-19} (47.5°C) [9]
Thickness d	bilayer thickness [Å] (head–head)	**47.9** (L_β', 20°) [56] 47.1 (L_β', 25°) [39] 47 (L_β', 30°) [72] 47.3 (P_β', 37°) [72]	**39.2** (L_β', 25°) [56] 43.1 (L_α, 45°) [72] 35.9 (L_α, 50°) [39]
	rel. thickness change main trans. $\Delta d/d$	**−0.163**[e]	
	thermal thickness exp. coefficient $D^{-1}\cdot(dD/dT)$ [K^{-1}][f]	**−0.00172**[f]	**−0.0016** (45°C)[f]

[a]Experimental results, this work.
[b]Calculated from values in this table.
[c]Values for DMPC.
[d]Taking area or thickness at indicated temperatures and correcting for the thermal expansion coefficients.
[e]Calculated from area and volume changes.
[f]Calculated from area and volume expansion coefficients. Bold values were used in calculations leading to Figs. 3–6.

changes, obtained by Nagle and Wilkinson [26] are within the margin of error identical, resulting in $\gamma^{vol} = 8.599 \times 10^{-4}$ cm^3/J (comparable to the value found for DMPC from the data in Fig. 1). This indicates that both pretransition and main transition are subject to volume fluctuations, resulting in changes of the elastic properties.

To calculate the volume compressibility $\kappa_T^{vol}(T)$, the heat capacity, ΔC_p, and the intrinsic compressibility, $\kappa_{T,0}^{vol}(T)$ (in the absence of isomerizational fluctuation), have to be obtained. Outside the transition range the latter can be obtained in densitometric experiments for gel and fluid phase independently, yielding $\kappa_{T,0}^{vol,gel}(T)$ and $\kappa_{T,0}^{vol,fluid}(T)$ [6,47].

The intrinsic compressibility in the transition range shall be approximated by

$$\kappa_{T,0}^{vol}(T) = (1-f)\cdot\kappa_{T,0}^{vol,gel}(T) + f\cdot\kappa_{T,0}^{vol,fluid}(T), \qquad (20)$$

where f is the fractional degree of melting as defined below. Experimental values for $\kappa_{T,0}^{vol,gel}(T)$ and $\kappa_{T,0}^{vol,fluid}(T)$ can be found in the literature (see Table 1). The fluid fraction, f, is defined to be proportional to the excess heat at a given temperature T and can be obtained from the heat capacity profile through

$$f = \frac{\Delta H(T)}{\Delta H_0} = \frac{\int_{T_1}^{T} \Delta C_p(T)dT}{\int_{T_1}^{T_2} \Delta C_p(T)dT}, \qquad (21)$$

where T_1 is a temperature below and T_2 is a temperature above the transition range.

Similarly, the intrinsic area compressibility can be deduced in analogy to Eq. 18 to yield

$$\kappa_{T,0}^{area}(T) = (1-f)\cdot\kappa_{T,0}^{area,gel}(T) + f\cdot\kappa_{T,0}^{area,fluid}(T) \qquad (22)$$

and the constants $\kappa_{T,0}^{area,gel}(T)$ and $\kappa_{T,0}^{area,fluid}(T)$ for DPPC can again be approximated by those for DMPC ([8]; see Table 1).

We will now translate the above considerations into numbers and compare them to experimental findings of other groups.

As an example we took the extruded DPPC LUV dispersions from Fig. 2. Using the literature values in Table 1, the heat capacity profiles were used to calculate the fractional degree of melting, the enthalpy, the temperature dependence of the volume, $\overline{V}$, the area, $\overline{A}$, and the membrane thickness, $\overline{D}$ (Fig. 3):

$$\overline{X}(T) = (1-f)\cdot\overline{X}_{gel}(T) + f\cdot\overline{X}_{fluid}(T) = \overline{X}_0(T) + f\cdot\Delta\overline{X}, \qquad (23)$$

where $\overline{X}$ is $\overline{V}$, $\overline{A}$ or $\overline{D}$.

The thermal thickness expansion coefficient was calculated from the volume and the area expansion coefficients, given as bold values in Table 1.

Using Eq. 12, it is possible to calculate the isother-

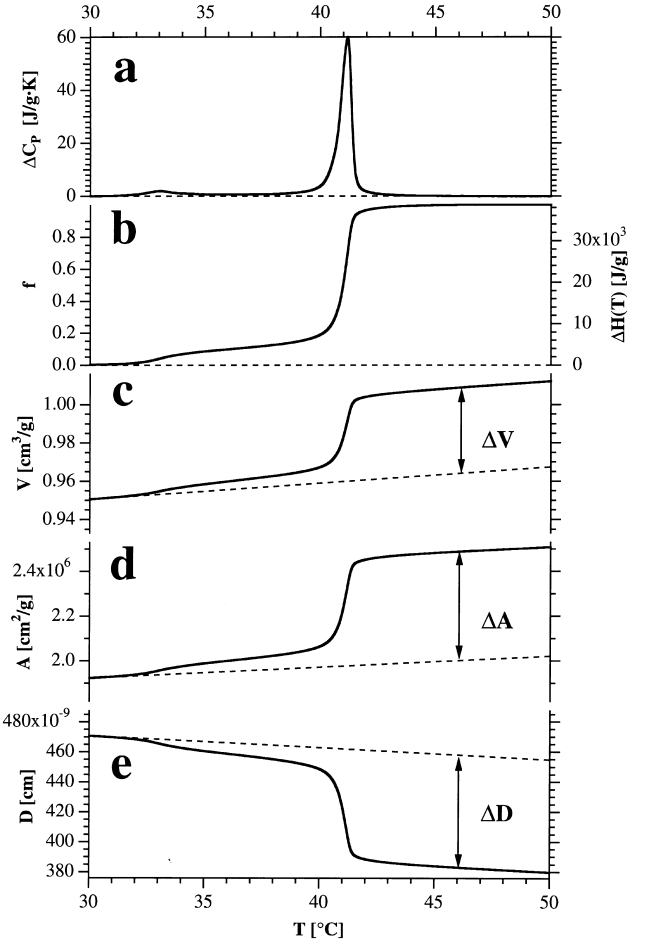

Fig. 3. Membrane dimensions of extruded DPPC LUV, calculated from the excess heat capacity. (a) Calorimetric excess heat capacity. (b) Fractional degree of melting, f, and excess enthalpy, ΔH, obtained from integrating the experimental ΔC_p profile. (c) Calculated temperature dependence of the membrane volume, V. (d) Calculated temperature dependence of the membrane area, A. (e) Calculated temperature dependence of the membrane thickness, D. The thickness is the headgroup to head group distance, ignoring water uptake of the surface in the ripple phase.

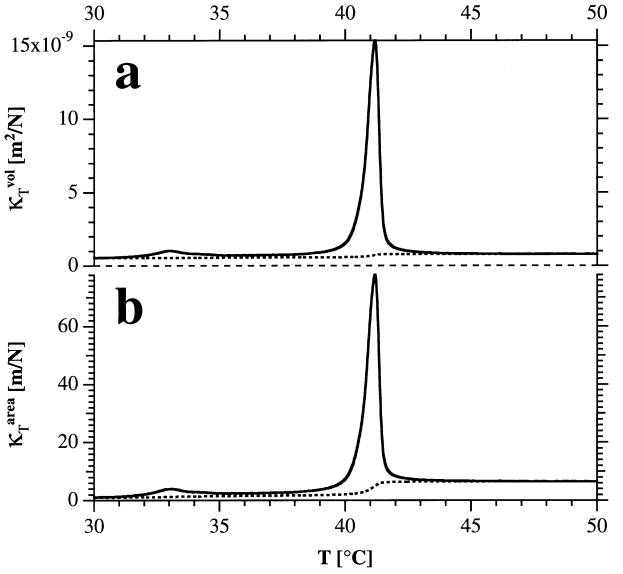

Fig. 4. Calculated isothermal volume compressibility (a) and calculated isothermal area compressibility (b), calculated for extruded DPPC LUV from the values in Fig. 3.

mal volume compressibility (Fig. 4, top) and area compressibility (Fig. 4, bottom), deduced from the proportionality relations between volume/area and enthalpy. The proportionality factors for DPPC are $\gamma_{vol} = 8.599 \times 10^{-4}$ cm^3/J and $\gamma_{area} = 8.93 \times 10^3$ cm^2/J. They both display a pronounced maximum in the transition range, showing a 10–20-fold increase in the transition range compared to the fluid phase compressibilities. The quantitative changes of the area compressibility are in the same order of magnitude as the changes determined by Evans and Kwok [7] for giant DMPC vesicles. Furthermore, a 7-fold increase of the volume compressibility of DPPC vesicles in the transition as compared to the fluid phase was found [47]. In the case of DPPC MLV one would expect a compressibility change which is about one order of magnitude larger than for the example given here.

One further method of obtaining information on critical phenomena of lipid dispersions is the measurement of the ultrasonic velocities [45,48]. We can use the above results to approximate the ultrasonic velocities in lipid dispersions.

Ultrasonic experiments are usually performed in the MHz regime with wavelength in the mm range. Since typical vesicle diameters are in the range of 0.1–1 μm, lipid dispersions may be considered to be homogeneous in ultrasonic experiments. The speed of sound in a homogeneous medium is given by

$$c_0 = \sqrt{\frac{1}{\rho \cdot \kappa_S^{vol}}} \tag{24}$$

where $\rho = m/V$ is the density and the mass m and the volume V are the sums of lipid and water mass and volume, respectively. Since the ultrasonic velocities in the literature are measured at high frequencies, we assumed that the lipid bilayers and the aqueous medium are adiabatically decoupled. Therefore we used Eqs. 17 and 18 to determine the adiabatic compressibility κ_S^{vol}.

Since the ultrasonic velocity of a lipid dispersion depends on the lipid concentration, it is convenient to use a sound velocity number defined as

$$u = \frac{c_0^{dispersion} - c_0^{H_2O}}{c_0^{H_2O} \cdot [L]} \tag{25}$$

where $[L]$ is the lipid concentration, usually given in mg/cm^3. If $u = 0$, the speed of sound in the lipids is equal to the speed of sound in water, which is in the range of 1500 m/s ($c_0^{H_2O}$ as a function of temperature is given by [49]). At low lipid concentrations, u is concentration-independent. In Fig. 5 the ultrasonic velocity number profiles are plotted as the function

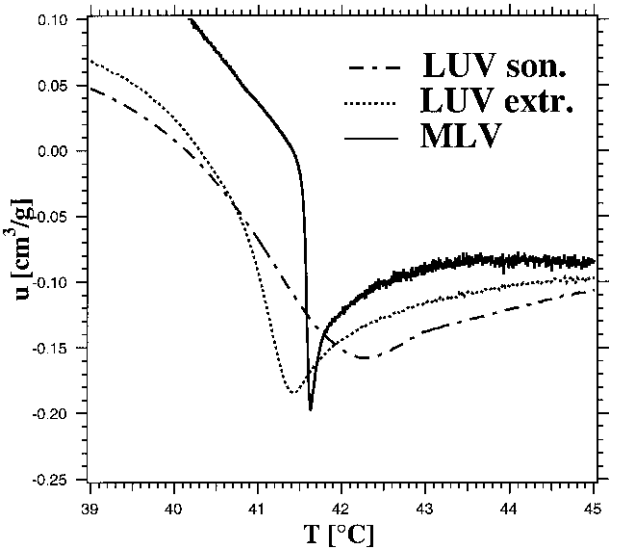

Fig. 5. Calculated sound velocity numbers for the three different DPPC vesicle preparations shown in Fig. 2. An adiabatic uncoupling of the membrane from the aqueous medium was assumed.

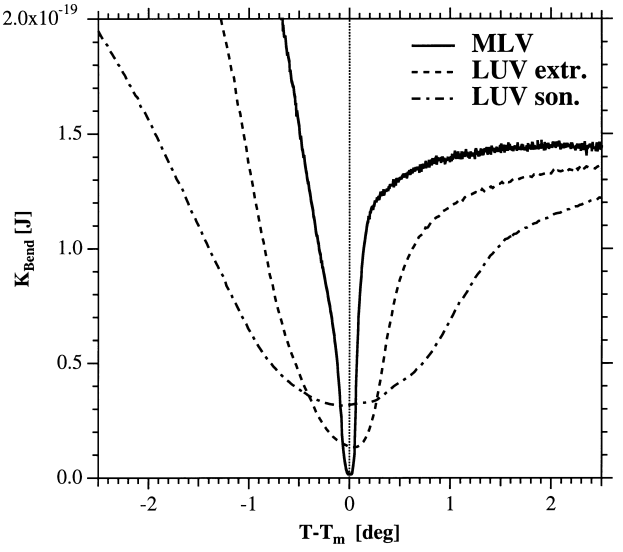

Fig. 6. Comparison of the elastic bending modulus of MLV, extruded LUV and sonicated LUV, calculated from the lateral area compressibility (Fig. 4b). The corresponding ΔC_p curves are given in Fig. 2. The absolute values for the extruded LUV are comparable to the changes found by Fernandez-Puente et al. [9] and Méléard et al. [5] for giant vesicles.

of temperature. The profiles were determined for the three different vesicle preparations. To be able to compare literature data [48] with the calculation, we used as intrinsic compressibilities $\kappa_{T,gel}^{vol} = 4.2 \times 10^{-10}$ cm^2/dyne and $\kappa_{T,fluid}^{vol} = 6.5 \times 10^{-10}$ cm^2/dyne, slightly lower but inside the margin of error similar to the values by Tosh and Collings [47]. The latter value is slightly lower than the isothermal compressibility determined by Liu and Kay [6]. The lipid heat capacity was taken to be $C_p = C_{p,0} + \Delta C_p$. The intrinsic heat capacity of the lipids $C_{P,0} = 1500$ cal/mol·deg was chosen to be close to that determined by Blume ([50], Table 1).

The results of this calculation are given in Fig. 5. A minimum of the velocity number u in the transition regime can be seen, caused by the compressibility maximum at the melting point. Since the cooperativity of MLV is much higher than for LUV (Fig. 2), the calculated ultrasonic velocity numbers of LUV lipid dispersions show a broadened, less pronounced minimum for large unilamellar vesicles. This has also been found experimentally by Mitaku et al. [48], who found a much broader sound velocity profile for sonicated small unilamellar vesicles than for multilamellar vesicles. The curves obtained by these authors are qualitatively and quantitatively comparable to the results given here. Since in Eq. 19 $C_{P,0}$ creates a kind of cutoff for the adiabatic compressibility, the sound velocity minima are quantitatively equally pronounced, in contrast to the magnitude of the heat capacity maxima. It should be noted that in the limit of zero frequency (complete relaxation in the isothermal limit), the minimum of the sound velocity number would be more pronounced by two orders of magnitude (data not shown).

The differences of the bending modulus, K_{bend}, in the main transition, expected for the three different types of DPPC vesicles shown in Fig. 2, are demonstrated in Fig. 6. The predicted decrease of K_{bend} for extruded vesicles is about 10-fold as compared to the fluid state. Fernandez-Puente et al. [9] and Méléard et al. [5] reported a pronounced decrease of the bending modulus by a factor of about 4–5 (approaching the melting points of DMPC and DPPC giant vesicles from temperatures above T_m) in the same order of magnitude as calculated here. No data were obtained below the melting point. Since the heat capacity of DPPC MLV in the transition is about 10-fold higher than ΔC_p of extruded LUV, the bending modulus is expected to be about 10 times smaller.

4. Discussion

In the present paper we discuss the consequences of the large enthalpy fluctuations in the lipid chain melting transition regime on the elastic properties of lipid membranes. This point of view is a macroscopic one, and the conclusions drawn are based on macroscopic fluctuations. Fluctuations on the molecular scale are taken as 'intrinsic' properties of the individual lipids. The theoretical findings of this work suggest that volume and area compressibilities as well as bending elasticities of membranes are simple functions of the excess heat capacity. Anthony et al. [27] have shown that for DMPC, DPPC and DMPC-DPPC mixtures the near proportional relation between excess volume changes and excess enthalpy changes is a very good approximation. This general result was found to be valid even in minute details of the melting process for extruded DMPC vesicles (Fig. 1). The proportionality relation formed the basis for the present description.

Pronounced maxima for the volume compressibility have experimentally been shown by means of ultrasonic velocity measurements [45] or high pressure experiments [6,47]. For the area compressibility they have been demonstrated using a pipette aspiration technique [7,8] and for membrane bending elasticities by flickering analysis of the membrane surface [5,9]. Mitaku et al. [48] found a broad minimum in the sound velocity numbers for DPPC small unilamellar vesicles and a much narrower minimum for the multilamellar vesicles. This is in agreement with the much smaller melting cooperativity in LUVs than in MLVs (compare Fig. 2).

The different transition half widths of the different vesicular preparations (Fig. 2) are probably a consequence of different surface curvature [51]. Additionally, bilayer-bilayer interactions may enhance the cooperativity in multilamellar vesicles. Whatever the exact origin of the different transition cooperativities, the conclusions drawn from the proportional relation between heat capacity and compressibilities are unaffected. It should be noted, however, that one cannot easily compare our calculations with experimental results from other sources, since different vesicle preparations yield different C_p profiles. The most reliable result is the one given in Fig. 1, where heat capacity and the temperature derivative of specific volume were obtained from the same vesicle preparation.

To calculate the lateral compressibility, the assumption was made that the heat obeys the same proportional relation to the area as it does to the volume. This is plausible, but the literature lacks data accurate enough to give definitive proof for this assumption. Even absolute numbers of lipid areas differ considerably. According to early papers [52,53] the area change for DPPC in the transition is about 17%, compensated by a decrease in membrane thickness, thereby resulting in the approximate volume change of 4% [26]. However, in contrast to the volume change, the exact magnitude of the area change is not clear. Absolute areas have been determined from X-ray as well as NMR experiments [54,55]. Numbers for the area are calculated indirectly from the experimental data and depend sensitively on the method used to analyze the data [54]. In the fluid phase areas between 57 Å^2 and 71 Å^2 have been reported. Rand and Parsegian [39] for example report areas for DPPC of 52 Å^2 at 25°C and 71 Å^2 at 50°C. This amounts to a relative area difference of 36%. The newest, most reliable result for the DPPC area is 62.9 Å^2 at 50°C [54,56] and 47.4 Å^2 at 25°C [56,57]. The calculation of relative area differences between gel and fluid states is complicated by the fact that the relative area change used in Eq. 7 is the area difference between gel and fluid phase at identical temperatures, whereas area values in the literature are often recorded at different temperatures. Corrected for the area expansion coefficient of about $(dA/dT)/A = 4\times10^{-3}$ K^{-1}, one arrives at a relative area change of 24.6% at the melting point. Needham and Evans [8], more directly, determined a relative area change of 22% for DMPC in the main transition using a pipette aspiration technique.

The thickness expansion coefficient has been calculated to be negative. This is a result of the relatively high area expansion coefficient reported by Needham and Evans [8] and Nagle et al. [57] (as compared to the volume expansion coefficient). The negative sign of the coefficient is probably a consequence of a change in the tilt angle of the lipids with temperature [57]. Absolute values for the thickness are used in the expression for the elastic bending modulus.

The elastic bending modulus may be calculated assuming that the fluctuations of the monolayers are mainly decoupled, meaning that the lateral compressibility of a bilayer is half that of a monolayer. This is not true if a coupling between the two monolayers exists, as recent statistical thermodynamics calculations suggest for lipid gel phases, where lipids are ordered on a hexagonal lattice in the membrane plane [58]. The relatively good quantitative agreement between the experimental data and the calculation in the fluid phase suggest, however, that this assumption may be a good one in the L_α phase, where this lateral order is lost.

A further assumption was the adiabatic uncoupling of membranes and water in the determination of the ultrasonic velocities. This assumption takes care of the reported slow relaxation of membrane processes in the melting regime, being in the second regime at the transition point of DPPC [44]. It leads to a good agreement with experimental data (Fig. 5; [48]) which made use of the isothermal compressibilities similar to those reported by Tosh and Collings [47]. In DMPC/cholesterol mixtures this was also

found to be true [45]. Heat diffusion of water, however, is very fast and one may argue that relaxation therefore should also be fast. The findings of our calculation suggest that the coupling between lipid chains and water is weak.

Evans and Kwok [7] tried to model the lateral compressibility maximum at the lipid melting transition by assuming first order transitional behavior with Gaussian temperature fluctuations around the melting point, leading to a broadening of the transition. To fit the experimental behavior, a phenomenological transition half width was introduced. The approach taken in the present paper is more general. Any effect that alters the heat capacity profiles is predicted to change the mechanical properties in a defined manner. It is known that secondary components like integral or peripheral proteins [20], but also cholesterol [59–61] or anesthetics [24,25,62], have pronounced effects on the excess heat capacity profiles of lipid membranes. Usually these components decrease the transition cooperativity and shift the transition maximum. Following the outline of this work, this is predicted to cause marked changes in the elastic constants. A recent study [45] has shown that the ultrasonic velocities in dispersions of DMPC-cholesterol systems have a close relation to the heat capacity profiles of those mixtures. Addition of cholesterol leads to a broadening of the transition profiles. At high cholesterol content ($>30\%$) no cooperative melting peak can be found. This is in good agreement with the absence of critical behavior in the bending modulus of DMPC-cholesterol membranes [5]. Melchior et al. [63] have studied the specific volume changes in the DPPC-cholesterol system, where the volume expansion coefficient displays close similarities with the heat capacity changes. In the present study we tried to calculate ultrasonic velocities in the special case of adiabatically decoupled membranes, meaning that compressional heat does not dissipate into the aqueous medium.

The bending of the membrane is linked to an elastic free energy change, which is dependent on the excess heat capacity. Therefore the work necessary to change the membrane morphology should be strongly temperature-dependent and is predicted to have a major influence on the equilibria between different vesicle states. To give an example of the relevance of this concept, let us assume a spherical vesicle filled with water, surrounded by a medium containing an osmotically active substance. The water inside the vesicle has a tendency to diffuse to the outside. Thus, a force acts on the vesicle, the tendency being to form an ellipsoidal or disk-like shape [35]. The stiffness of the membrane, however, favors a spherical shape [34]. Close to the melting point of the vesicle the bending elasticity is greatly enhanced and the equilibrium between spherical and flat vesicles is shifted away from the spherical shapes. Therefore, structural transitions of vesicles may be induced by the thermotropic melting transition. A related transition of this kind was theoretically described by Damman et al. [34], who called this kind of structural change an inflation-deflation transition. These transitions require competition between the elastic free energy of bending and a driving force that favors a curved membrane. The latter force may, as mentioned above, consist of an osmotic pressure difference, but also of hydrational effects on the surface, or electrostatic contributions. Furthermore, the marked increase of the bending elasticity in the melting regime may give rise to large curvature undulations [31]. Such undulations have experimentally been demonstrated to exist in the lipid melting regime in neutron scattering experiments on DMPC and DPPC multilayers [32], although the effect for the latter was not very pronounced. This may be due to the very small transition half width (0.055° for DPPC), making it very difficult to take precise measurements at the melting point. Also, there may be some coupling of the monolayers leading to a partial suppression of the undulations.

The bending of a membrane is linked to an expansion of the outer and a compression of the inner monolayer. According to the Clausius-Clapeyron principle the melting points of a membrane are linked to lateral pressure through $dT_m/d\Pi = T_m \cdot \Delta A/\Delta H$ [27]. Therefore the bending of a membrane will cause the melting profiles to alter. On bending, the outer monolayer transitional events are shifted to lower temperatures, whereas the melting events in the inner monolayer are shifted to higher temperatures, thus giving rise to an overall broadening of the transition profile. This is evident for example in the calorimetric curves of Fig. 2, where sonicated LUV display a larger transition half width than extruded LUV and MLV, leaving the transition point almost

unaffected. A broadening upon bending has also been demonstrated for membranes supported by beads of different diameter [51]. The elastic bending modulus can be calculated from Eq. 15 in the limit of very small curvature only, since the bending distorts the calorimetric melting profile and therefore the bending modulus. Statistical thermodynamics calculations are required to determine the bending energy of a strongly curved membrane segment. Such calculations will have to take into account that the two monolayers are no longer uncoupled. This will be done in a future publication (in preparation).

Nevertheless, structural transitions that involve changes in mean curvature, and which are linked to lipid chain melting in lipid membranes, will become evident in the melting profiles of a lipid vesicle [64]. Such changes have been seen for example in dimyristoyl glycerol vesicles at low ionic strength [65]. In this system, a transformation between spherical vesicles and an extended membrane network occurs [66]. These changes are accompanied by a complex excess heat capacity profile with three maxima, being closely related to the structural changes. A further heat capacity anomaly is the lipid pretransition, where ripple formation gives rise to an additional heat capacity maximum (pretransition) at temperatures slightly lower than the main transition [2,52]. Recently, a heat capacity anomaly at the lower end of the main transition of long chain phosphatidylcholines, called sub-main transition, was reported [67,68].

Finally one may speculate about the possibility of the existence of mechanical excitations in the membrane plane [69]. From the present investigation, it is unclear whether a sound wave may propagate over a long distance without significant loss in energy. However, lateral speeds of sound in the limit of complete relaxation (calculated data not shown, see [21]) are in the same order of magnitude as the nerve excitation velocity (77 m/s in the transition of extruded DPPC LUV, 5–25 m/s in squid giant axons, about 100 m/s in myelinated nerves). It is known, on the other hand, that the nerve pulse is accompanied by a mechanical displacement of the surface, which is strongly correlated with the action potential [70]. During the action potential an adiabatic temperature response was found [71]. Thus, mechanical changes of the nerve membrane take place during the nerve pulse. Therefore, changes of mechanical membrane properties may have an influence on the propagation of the action potential.

We conclude that the findings of this paper may help to investigate the curvature dependence of heat capacity profiles and to understand morphological changes close to the lipid melting regime. The proportionality relation between volume and enthalpy is a helpful tool to estimate the elastic properties of membranes.

Acknowledgements

I am very grateful to Holger Ebel from our laboratory for letting me use one of his data sets (in Fig. 1) prior to publication, and to Michaela Hoeckel for letting me use her heat capacity profile of extruded DPPC vesicles. Anthony Streeter was so kind to read and correct my manuscript. I furthermore thank Dr. Tom Jovin for granting me permission to perform calorimetric experiments on his micro-calorimeter. This project was supported by a grant from the Deutsche Forschungsgemeinschaft (DFG).

Appendix A

Experimentally it is found that $\overline{\Delta V} = \gamma^{\mathrm{vol}}\overline{\Delta H}$ ([27]; Fig. 1) around the melting transition of single lipids and lipid mixtures. Let us assume that this is true at all temperatures.

$$\overline{\Delta V} = \frac{1}{Q}\cdot\sum_{\mathrm{i}}\Delta V_{\mathrm{i}}\cdot\Omega_{\mathrm{i}}\exp\left(-\frac{H_{\mathrm{i}}}{RT}\right) =$$

$$\frac{\gamma^{\mathrm{vol}}}{Q}\cdot\sum_{\mathrm{i}}\Delta H_{\mathrm{i}}\cdot\Omega_{\mathrm{i}}\exp\left(-\frac{H_{\mathrm{i}}}{RT}\right) =$$

$$\frac{1}{Q}\cdot\sum_{\mathrm{i}}(\gamma^{\mathrm{vol}}\Delta H_{\mathrm{i}})\cdot\Omega_{\mathrm{i}}\exp\left(-\frac{H_{\mathrm{i}}}{RT}\right)\ ,\quad 0\leq T\leq\infty.$$

If $0\leq 1/RT\leq\infty$, the $\exp(-\Delta H_{\mathrm{i}}/RT)$ form a set of basis functions of a Laplacian space with the variable $1/RT$. This implies that the set of pre-factors $\gamma^{\mathrm{vol}}\cdot\Delta H_{\mathrm{i}}\cdot\Omega_{\mathrm{i}}$ is well defined and unique. The Ω_{i} are temperature-independent and constant. Therefore not only $\overline{\Delta V} = \gamma^{\mathrm{vol}}\overline{\Delta H}$, but also $\Delta V_{\mathrm{i}} = \gamma^{\mathrm{vol}}\Delta H_{\mathrm{i}}$ for

all available (!) substates of the system. Consequently also $\Delta H_i^2 = (\gamma^{vol}\Delta H_i)^2$ and

$$\overline{\Delta V^2} = \frac{1}{Q}\cdot\sum_i (\gamma^{vol}\Delta H_i)^2\cdot\Omega_i \exp\left(-\frac{H_i}{RT}\right) = (\gamma^{vol})^2\overline{\Delta H^2},$$

which had to be shown. Therefore

$$(\overline{\Delta V^2} - \overline{\Delta V}^2) = (\gamma^{vol})^2(\overline{\Delta H^2} - \overline{\Delta H}^2)$$

This is a non-trivial statement, which is not strictly true if the proportionality relation does not hold at all temperatures. It is approximately true in the transition range, if this relation is valid in a reasonable interval around the phase transition.

References

[1] T. Hianik, V.I. Passechnik, Bilayer Lipid Membranes: Structure and Mechanical Properties, Kluwer Academic, Dordrecht, 1995.
[2] D. Marsh, CRC Handbook of Lipid Bilayers, CRC Press, Boca Raton, FL, 1990.
[3] E. Sackmann, FEBS Lett. 346 (1994) 3–6.
[4] H. Strey, M. Peterson, E. Sackmann, Biophys. J. 69 (1995) 478–488.
[5] P. Méléard, C. Gerbeaud, T. Pott, L. Fernandez-Puente, I. Bivas, M.D. Mitov, J. Dufourcq, P. Bothorel, Biophys. J. 72 (1997) 2616–2629.
[6] N.-I. Liu, R.L. Kay, Biochemistry 16 (1977) 3484–3486.
[7] E.A. Evans, R. Kwok, Biochemistry 21 (1982) 4874–4879.
[8] D. Needhamn, E. Evans, Biochemistry 27 (1988) 8261–8269.
[9] L. Fernandez-Puente, I. Bivas, M.D. Mitov, P. Méléard, Europhys. Lett. 28 (1994) 181–186.
[10] D.A. Pink, D. Chapman, Proc. Natl. Acad. Sci. USA 76 (1979) 1542–1546.
[11] O.G. Mouritsen, Ann. NY Acad. Sci. 491 (1986) 166–169.
[12] O.G. Mouritsen, in: R. Brasseur (Ed.), Computer Simulation of Cooperative Phenomena in Lipid Membranes, CRC Press, Boca Raton, FL, 1989.
[13] O.G. Mouritsen, Chem. Phys. Lipids 57 (1991) 179–194.
[14] Z. Zhang, M.J. Zuckermann, O.G. Mouritsen, Phys. Rev. A 46 (1992) 6707–6713.
[15] D.P. Fraser, M.J. Zuckermann, O.G. Mouritsen, Phys. Rev. A 43 (1991) 6642–6656.
[16] J. Risbo, M.M. Sperotto, O.G. Mouritsen, J. Chem. Phys. 103 (1995) 3643–3656.
[17] O.G. Mouritsen, R.L. Biltonen, in: A. Watts (Ed.), New Comprehensive Biochemistry, Protein Lipid Interactions, Elsevier, Amsterdam, 1992.
[18] M.M. Sperotto, O.G. Mouritsen, Biophys. J. 59 (1991) 261.
[19] M.M. Sperotto, O.G. Mouritsen, Eur. Biophys. J. 22 (1993) 323–328.
[20] T. Heimburg, R.L. Biltonen, Biophys. J. 70 (1996) 84–96.
[21] T. Heimburg, D. Marsh, in: B. Roux, K.M. Merz (Eds.), Biological Membranes – A Molecular Perspective from Computation and Experiment, Birkhäuser, Boston, MA, 1996.
[22] L. Cruzeiro-Hansson, J.H. Ipsen, O.G. Mouritsen, Biochim. Biophys. Acta 979 (1990) 166–176.
[23] I.P. Sugar, R.L. Biltonen, N. Mitchard, in: L. Brand, M.L. Johnson (Eds.), Methods in Enzymology, Vol. 240, Academic Press, New York, 1994.
[24] O.G. Mouritsen, K. Jørgensen, Mol. Membr. Biol. 12 (1995) 15–20.
[25] D.B. Mountcastle, R.L. Biltonen, M.J. Halsey, Proc. Natl. Acad. Sci. USA 75 (1978) 4906–4910.
[26] J.F. Nagle, D.A. Wilkinson, Biophys. J. 23 (1978) 159–175.
[27] F.H. Anthony, R.L. Biltonen, E. Freire, Anal. Biochem. 116 (1981) 161–167.
[28] T.L. Hill, An Introduction to Statistical Mechanics, Dover, New York, 1960.
[29] W. Helfrich, Z. Naturforsch. 28c (1973) 693–703.
[30] F.C. Frank, Discuss. Faraday Soc. 25 (1958) 19–281.
[31] W. Helfrich, Z. Naturforsch. 33a (1978) 305–315.
[32] T. Hønger, K. Mortensen, J.H. Ipsen, J. Lemmich, R. Bauer, O.G. Mouritsen, Phys. Rev. Lett. 72 (1994) 3911–3914.
[33] O.G. Mouritsen, P.K.J. Kinnunen, in: B. Roux, K.M. Merz (Eds.), Biological Membranes – A Molecular Perspective from Computation and Experiment, Birkhäuser, Boston, MA, 1996.
[34] B. Dammann, H.C. Fogedby, J.H. Ipsen, C. Jeppesen, J. Phys. I. France 4 (1994) 1139–1149.
[35] U. Seifert, R. Lipowski, in: R. Lipowski, E. Sackmann (Eds.), Handbook of Biological Physics, Elsevier, Amsterdam, 1995.
[36] W. Helfrich, Z. Naturforsch. 29c (1974) 510–515.
[37] R. Lumry, R.B. Gregory, in: G.R. Welch (Ed.), The Fluctuating Enzyme, John Wiley and Sons, New York, 1986.
[38] A.H. Wilson, Thermodynamics and Statistical Mechanics, Cambridge University Press, Cambridge, 1957.
[39] R.P. Rand, V.A. Parsegian, Biochim. Biophys. Acta 988 (1989) 351–376.
[40] E.A. Evans, Biophys. J. 14 (1974) 923–931.
[41] D.R. Lide, H.P.R. Frederikse, Handbook of Chemistry and Physics, 77th edn. 1996–97, CRC Press, Boca Raton, FL, 1996.
[42] G. Beggerow, Landolt/Börnstein IV: High Pressure Properties of Matter, Springer, Berlin, 1980.
[43] W.W. van Osdol, R.L. Biltonen, M.L. Johnson, J. Biochem. Biophys. Methods 20 (1989) 1–46.
[44] W.W. van Osdol, M.L. Johnson, Q. Ye, R.L. Biltonen, Biophys. J. 59 (1991) 775–785.
[45] S. Halstenberg, T. Heimburg, T. Hianik, U. Kaatze, R. Krivanek, Biophys. J. 75 (1998) 264–271.
[46] A.J. Jin, C.P. Mudd, N.L. Gershfeld, Biophys. J. 74 (1998) A312.
[47] R.E. Tosh, P.J. Collings, Biochim. Biophys. Acta 859 (1986) 10–14.

[48] S. Mitaku, A. Ikegami, A. Sakanishi, Biophys. Chem. 8 (1978) 295–304.
[49] N. Bilaniuk, G.S.K. Wong, J. Acoust. Soc. Am. 93 (1993) 1609–1612.
[50] A. Blume, Biochemistry 22 (1983) 5436–5442.
[51] T. Brumm, K. Jørgensen, O.G. Mouritsen, T.M. Bayerl, Biophys. J. 70 (1996) 1373–1379.
[52] M.J. Janiak, D.M. Small, G.G. Shipley, Biochemistry 15 (1976) 4575–4580.
[53] M.J. Janiak, D.M. Small, G.G. Shipley, J. Biol. Chem. 254 (1979) 6068–6078.
[54] J.F. Nagle, Biophys. J. 64 (1993) 1476–1481.
[55] B.W. Koenig, H.H. Strey, K. Gawrisch, Biophys. J. 73 (1997) 1954–1966.
[56] J.F. Nagle, R. Zhang, S. Tristam-Nagle, W. Sun, H.I. Petrache, Biophys. J. 70 (1996) 1419–1431.
[57] W.J. Sun, S. Tristam-Nagle, R.M. Suter, J.F. Nagle, Biophys. J. 71 (1996) 885–891.
[58] M. Nielsen, L. Miao, J.H. Ipsen, O.G. Mouritsen, M.J. Zuckermann, Phys. Rev. A 54 (1996) 6889–6905.
[59] S. Mabrey, P.L. Mateo, J.M. Sturtevant, Biochemistry 17 (1978) 2464–2468.
[60] E. Sackmann, in: R. Lipowski, E. Sackmann (Eds.), Handbook of Biological Physics, Elsevier, Amsterdam, 1995.
[61] T.P.W. McMullen, R.N. McElhaney, Biochim. Biophys. Acta 1234 (1995) 90–98.
[62] W.W. van Osdol, Q. Ye, M.L. Johnson, R.L. Biltonen, Biophys. J. 63 (1992) 1011–1017.
[63] D.L. Melchior, F.J. Scavitto, J.M. Steim, Biochemistry 19 (1980) 4828–4834.
[64] T. Heimburg, Biophys. J. 72 (1997) A132.
[65] T. Heimburg, R.L. Biltonen, Biochemistry 33 (1994) 9477–9488.
[66] W. Jahn, B. Kloesgen, T. Heimburg, Biophys. J. 74 (1998) A13.
[67] K. Jørgensen, Biochim. Biophys. Acta 1240 (1995) 111–114.
[68] M. Nielsen, L. Miao, J.H. Ipsen, K. Jorgensen, M.J. Zuckermann, O.G. Mouritsen, Biochim. Biophys. Acta 1283 (1996) 170–176.
[69] K. Kaufmann, The Lipid Membrane, Caruaru, Brazil, 1989.
[70] I. Tasaki, K. Iwasa, R.C. Gibbons, Jpn. J. Physiol. 30 (1980) 897–905.
[71] J.M. Ritchie, R.D. Keynes, Q. Rev. Biophys. 18 (1985) 451–470.
[72] Y. Inoko, T. Mitsui, J. Phys. Soc. Japan 44 (1978) 1918–1924.